clearly indicate that the extra peaks originate from coordinated citrates and that the citrates are released to be averaged on the NMR time scale, when a sufficient amount of citrate (cit:Bi > 1:1) is present in the system. In fact, for the all other bismuth citrate compounds (**1**, **2a**, **2b**, **3a**, and **5**) whose citrate:bismuth ratios are higher than 1.0, all citrates average on the NMR time scale under low-concentration conditions, as mentioned above.

According to the elemental analyses, **4a** and **4b** seem to contain $[Bi-O(H)-Bi]_n$ units. The hydrolysis of Bi(III) has been extensively studied and the predominance of several hexanuclear species, such as $[Bi_6O_4(OH)_4]^{6+}$, in acidic solutions is well established.[29,30] If the presence of such hexanuclear species is assumed for the solutions of **4a** and **4b**, then the behavior can be explained well. Since the hexanuclear unit decomposes in basic conditions, the "isolated" bismuth ions will be able to react with citrates, which exchange rapidly on the NMR time scale just like the other bismuth citrate compounds. An excess of citrate may coordinate with such a unit, so as to weaken and destroy the Bi-O bonds that are frameworks in a hexanuclear cluster. Although the structure determination of compound **4** as a solid has been attempted, this was unsuccessful so far, due to the poor quality of the crystals.

Concluding Remarks

In this investigation, five types of solid compounds were synthesized by varying the $Bi:H_4cit:KOH:NH_4OH$ ratio. In the case of two compounds, i.e. **1** and **5**, a 3-D structure could be determined by using X-ray diffraction on single crystals. For the citrate anion, whether in triionized or tetraionized form, tridentate chelation to Bi(III) is evident. Only in the case of compound **4**, prepared with a small excess of citrate, are not all Bi ions tridentately chelated by citrate (ratio Bi:citrate = 3:2), and a cluster structure, such as $[Bi_6O_4(OH)_4(Hcit)_4]^{6-}$, appears likely.

To the best of our knowledge, the rapid ligand exchange of citrates is unprecedented for bismuth. On the other hand, in solutions with high concentration that are attained only under basic conditions, citrates coordinate to bismuth rigidly, to yield oligomeric or polymeric units. Exceptionally, compounds **4a** and **4b** show separate signals for free and coordinated citrates in their ^1H NMR spectra even in low concentration. Although the reason is not clear at this stage, a plausible explanation is given by existence of $[Bi-O(H)-Bi]_n$ units in the solid form. The most plausible candidate for the unit is a well-established hexanuclear cluster $[Bi_6O_4(OH)_4]^{6+}$.[27,28] In that case compound **4** should be described as $(NH_4)_xK_{6-x}[Bi_6O_4(OH)_4(Hcit)_4](H_2O)_8$ in the solid state.

Note Added in Proof. After the acceptance of this paper, a communication has appeared in this journal,[33] dealing with the crystal structure of $KBi(C_6H_4O_7)\cdot 3H_2O$, ($KBi(cit^{4-})\cdot 3H_2O$) a compound close in analyses (though not identical) to our compounds **2** and **3**. Although these authors used ammonia for growth of the crystals, they did not give a K/NH_4 ratio. The structure of their compound also contains the Bi(cit) units in which cit^{4-} is tridentate chelating to Bi(III), with a short Bi-O3 distance, just as found in our compounds **1** and **5**. No Bi-Bi distances were given.

Acknowledgment. We are indebted to Mr. S. Gorter for collecting the X-ray data sets. Drs. J. W. Groenendaal, C. M. Hol, N. T. M. Klooster, and J. Raaijmakers (Gist-brocades, Delft, The Netherlands) are thanked for many useful discussions. Financial support of Gist-brocades is gratefully acknowledged.

Registry No. **5**, 136445-28-8; KBi(cit), 136445-27-7.

Supplementary Material Available: A figure showing the NMR spectrum of compound **4a** and tables of bond lengths and bond angles, of fractional coordinates of the hydrogen atoms, and of anisotropic thermal parameters of the non-hydrogen atoms (13 pages); listings of structure factors (67 pages). Ordering information is given on any current masthead page.

(28) As the citrate:bismuth ratio increases, the pH* value increases. Resultant pH* values for each citrate:bismuth ratio are as follows: pH* 6.96 for cit:Bi = 2:3 (without addition of free citrate), pH* 7.18 for 3:3, pH* 7.25 for 4:3, pH* 7.29 for 5:3, and pH* 7.31 for 6:3.
(29) Baes, C. F., Mesmer, L. G., Eds. *The Hydrolysis of Cations*; Wiley: New York, 1976.
(30) Sundvall, B. *Inorg. Chem.* **1983**, *22*, 1906 and references cited therein.
(31) Weast, R. C. *Handbook of Chemistry and Physics*, 66th ed.; CRC Press, Inc.: Boca Raton, FL, 1986.
(32) For example, a type **1** compound was obtained by concentrating the filtrate from which **3b** was removed. When methanol vapor was diffused into the filtrate from which **2b** was removed, type **4** was obtained.
(33) Herrmann, W. A.; Herdtweck, E.; Pajdla, L. *Inorg. Chem.* **1991**, *30*, 2581-2582.

Contribution from the Department of Applied Chemistry, Faculty of Engineering, Kumamoto University, Kurokami, Kumamoto 860, Japan, and Institute for Molecular Science, Okazaki 444, Japan

Ethylene, Silene, and Disilene Coordinate Bonds with Platinum(0) and Platinum(II). An ab Initio MO/MP4 and SD-CI Study

Shigeyoshi Sakaki*,[1] and Masami Ieki

Received January 4, 1991

$[PtCl_3L]^-$ and $Pt(PH_3)_2L$ (L = C_2H_4, SiH_2CH_2, or Si_2H_4) are investigated with ab initio MO/MP4 and SD-CI methods. Binding energies of these complexes increase in the order ethylene < silene < disilene in both Pt(0) and Pt(II) complexes, and their coordinate bonds are stronger in Pt(II) complexes than in Pt(0) complexes. The disilene coordinate bond of $Pt(PH_3)_2(Si_2H_4)$ can be described as a three-centered metallocyclopropane type interaction, while the ethylene coordinate bond of $[PtCl_3(C_2H_4)]^-$ and $Pt(PH_3)_2(C_2H_4)$ exhibits the character of C=C double-bond coordination. Electron correlation has little effect on geometries of these complexes but has a significant influence on binding energies.

Introduction

Transition-metal complexes with silene and disilene are of considerable interest in the chemistry of Si compounds[2] because coordination to transition metals is one useful way to stabilize such reactive species as silene and disilene. In this regard, several transition-metal complexes of silene and disilene have been reported in recent studies.[3] However, very little has been known regarding the coordinate bond nature and the electronic structure of transition-metal complexes of silene and disilene, and only one theoretical study of a disilene complex has been reported,[4] to our knowledge.

(1) S.S. is a visiting professor of Institute for Molecular Science from Kumamoto University.
(2) For instance, West, R. *Angew. Chem., Int. Ed. Engl.* **1987**, *26*, 1201.
(3) (a) Campion, B. K.; Heyn, R. H.; Tilley, T. D. *J. Am. Chem. Soc.* **1988**, *110*, 7558. (b) Zarate, E. A.; Tessier-Youngs, C. A.; Youngs, W. J. *J. Am. Chem. Soc.* **1988**, *110*, 4068. (c) Pham, E. K.; West, R. *J. Am. Chem. Soc.* **1989**, *111*, 7667. (d) Pham, E. K.; West, R. *Organometallics* **1990**, *9*, 1517. (e) Berry, D. H.; Chey, J. H.; Zipin, H. S.; Carroll, P. J. *J. Am. Chem. Soc.* **1990**, *112*, 452.
(4) Anderson, A. B.; Shiller, P.; Zarate, E. A.; Tessier-Youngs, C. A.; Youngs, W. J. *Organometallics*, **1989**, *8*, 2320.

0020-1669/91/1330-4218$02.50/0

Chart I

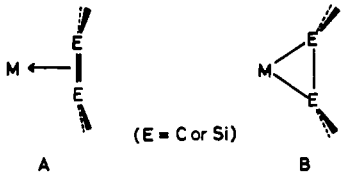

In this work, ethylene, silene, and disilene complexes of Pt(0) and Pt(II), $Pt(PH_3)_2L$ and $[PtCl_3L]^-$ (L = C_2H_4, SiH_2CH_2, Si_2H_4), are investigated theoretically with ab initio MO/MP4 and SD–CI methods. These complexes are selected here as good examples of silene and disilene complexes because a Pt(0)–disilene complex has been recently isolated[3c,d] and the similar ethylene complexes $Pt(PH_3)_2(C_2H_4)$ and $[PtCl_3(C_2H_4)]^-$, have been well investigated as typical transition-metal–olefin complexes.[5] Through this theoretical work, we hope to discuss mainly the following two issues; the first is how the coordinate bond nature and electron distribution of silene and disilene complexes are characterized, compared to their ethylene analogues, and the second is how much electron correlation influences the geometry and the binding energy. It is our intention with this work to estimate semiquantitatively the binding energies of silene and disilene complexes with Pt(0) and Pt(II) and to elucidate whether a coordinate bond of disilene in $Pt(PH_3)_2(Si_2H_4)$ should be described as Si=Si double bond coordination (Chart IA) or as a three-centered metallocyclopropane type interaction (Chart IB).

Computational Details

Ab initio closed-shell Hartree–Fock and MP4 calculations were carried out with the Gaussian 82 program,[6] and SD–CI calculations were performed with the MELD program.[7] Two kinds of basis sets, BS-I and BS-II, were employed. The BS-I set was used only in geometry optimization at the Hartree–Fock level, and the BS-II set was employed in MP4 and SD–CI calculations. In BS-I, the 5s, 5p, 5d, 6s, and 6p orbitals of Pt were represented by a (5s 5p 3d) primitive set contracted to [3s 3p 2d],[8] where inner core orbitals of Pt were replaced by a relativistic effective core potential.[8] For ligand atoms, MIDI-3 basis sets were used,[9a,b] except for MINI-1 sets used for a PH_3 group.[9a] The basis set of Si was augmented with a d-polarization function.[9c] In BS-II, the 5s, 5p, 5d, 6s, and 6p orbitals of Pt were represented by the same primitive set of (5s 5p 3d) as in the BS-I set, but a more flexible contraction of [3s 3p 3d] was adopted. For all other atoms, MIDI-4 sets were used, where the same d-polarization function as in the BS-I basis was added to a Si basis set.[9c]

Geometry optimization was carried out with an energy gradient method at the Hartree–Fock level, where the geometry of PH_3 was taken from the experimental structure of the free PH_3 molecule[10] and fixed during the optimization. In MP4 calculations, all core orbitals were excluded from an active space. SD–CI calculations were performed with a single Hartree–Fock configuration as the reference, where all core orbitals were excluded from the active space and virtual orbitals were transformed to K-orbitals to improve the CI convergence.[11] All possible single and double excited configurations were screened, based on the Rayleigh–Schrödinger perturbation theory (energy threshold = 5.0×10^{-5} hartrees).[12] The resultant excited configurations underwent a variational CI calculation.[13] The variationally calculated limited SD–CI correlation energy, E(lim SD–CI), was corrected by estimating the correlation energy arising from configurations discarded by the perturbation selection, to give E(est SD–CI),[14] and then this value was further corrected by incorporating correlation energy arising from higher order CI expansions, to yield E(est full CI).[15]

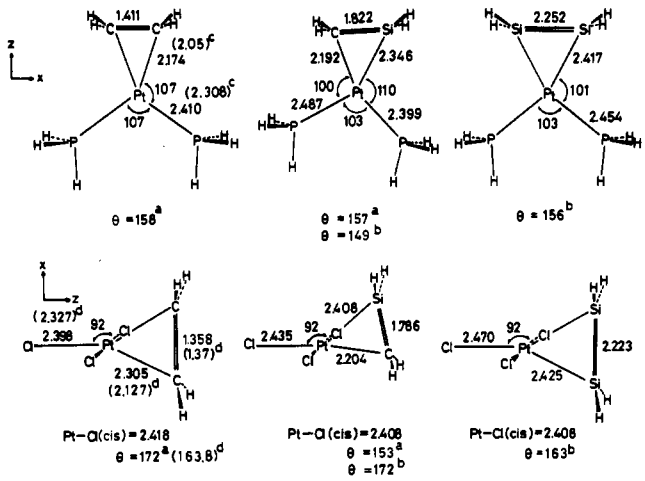

Figure 1. Optimized structures of $Pt(PH_3)_2L$ and $[PtCl_3L]^-$ (L = C_2H_4, SiH_2CH_2, Si_2H_4) (distances in Å and angles in deg): (a) CH_2 back-bending angle; (b) SiH_2 back-bending angle. (c) experimental values for $Pt(PPh_3)_2(Cl_2C{=}CF_2)$[17a]; (d) averaged experimental values for $K[PtCl_3(C_2H_4)]$.[16a]

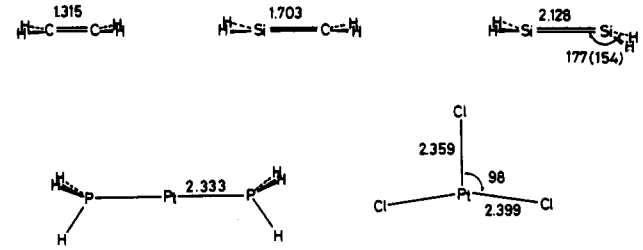

Figure 2. Optimized structures of metal fragments and ligands (distances in Å and angles in deg). In parentheses is given the optimized value at the MP2 level.

Results and Discussion

Geometries at the Hartree–Fock Level. Optimized structures of $[PtCl_3L]^-$ and $Pt(PH_3)_2L$ (L = C_2H_4, SiH_2CH_2, Si_2H_4) are shown in Figure 1 and those of metal fragments and free ligands are given in Figure 2. Let us compare the optimized structures of $Pt(PH_3)_2(C_2H_4)$ and $[PtCl_3(C_2H_4)]^-$ with experimental ones at first, because structures of these complexes have been well investigated.[16,17] In $[PtCl_3(C_2H_4)]^-$, the C=C bond is calculated to lengthen by ca. 0.043 Å upon C_2H_4 coordination to a similar

(5) (a) For instance, Hartley, F. R. In *Comprehensive Organometallic Chemistry*; Wilkinson, G., Ed.; Pergamon Press: Oxford, England, 1982; Vol. 6, p 471. (b) Ziegler, T.; Rauk, A. *Inorg. Chem.* **1979**, *18*, 1558. (c) Ziegler, T. *Inorg. Chem.* **1985**, *24*, 1547. (d) Albright, T. A.; Hoffmann, R.; Thibeault, J. C.; Thorn, D. A. *J. Am. Chem. Soc.* **1979**, *101*, 3801. (e) Hay, P. J. *J. Am. Chem. Soc.* **1981**, *103*, 1390.

(6) Binkley, J. S.; Frisch, M.; Raghavachari, K.; Defrees, D.; Schegel, H. B.; Whiteside, R.; Fluder, E.; Seeger, R.; Pople, J. A. *Gaussian 82*; Carnegie-Mellon Quantum Chemistry Archive; Carnegie-Mellon University: Pittsburgh, PA, 1983. Several routines for effective core potential calculations supplied by P. J. Hay have been added to this program by Dr. N. Koga and Prof. K. Morokuma.

(7) Davidson, E. R.; McMurchie, L.; Elbert, S. R.; Langhoff, S. R.; Rawlings, D.; Feller, D. *Program, MELD*; University of Washington: Seattle, WA, IMS Computer Library, No. 030.

(8) Hay, P. J.; Wadt, W. R. *J. Chem. Phys.* **1985**, *82*, 299.

(9) (a) Huzinaga, S.; Anzelm, J.; Kłobukowski, M.; Radzio-Andzelm, E.; Sakai, Y.; Tatewaki, H. *Gaussian basis sets for molecular calculations*; Elsevier: Amsterdam, 1984. (b) For the H atom: Dunning, T. H. *J. Chem. Phys.* **1970**, *53*, 2823. (c) Sakai, Y.; Tatewaki, H.; Huzinaga, S. *J. Comput. Chem.* **1981**, *2*, 108.

(10) Herzberg, G. *Molecular Spectra and Molecular Structure*; D. Van Nostrand, Co.: Princeton, NJ, 1967; Vol. 3, p 610.

(11) Feller, D.; Davidson, E. R. *J. Chem. Phys.* **1981**, *84*, 3997.

(12) (a) Langhoff, S. R.; Davidson, E. R. *Int. J. Quantum. Chem.* **1974**, *8*, 61. (b) The configuration functions that underwent a variational SD-CI calculations include over 90% of the estimated single and double excited correlation energy.

(13) C_0 is about 0.92 in all the complexes examined.

(14) E_r (est SD–CI) = $E_0 + [E_r(\text{lim SD–CI}) - E_0](1 + E_{disc}/E_{kept})$, where E_{disc} and E_{kept} are the SD correlation energy excluded and that included in the variational SD–CI calculations, respectively, and E_0 is the total energy at the Hartree-Fock level. Both E_{disc} and E_{kept} are estimated by the second-order Rayleigh–Schrödinger perturbation method.[12a]

(15) Davidson, E. R.; Silver, D. W. *Chem. Phys. Lett.* **1977**, *52*, 403.

(16) (a) Love, R. A.; Koetzle, T. F.; Williams, G. J. B.; Andrews, L. C.; Bau, R. *Inorg. Chem.* **1975**, *14*, 2653 and references cited therein. (b) Jarvis, J. A. J.; Kilbourn, B. T.; Owston, P. G. *Acta Crystallogr.* **1971**, *B27*, 366; **1970**, *B26*, 876. (c) Black, M.; Mais, R. H. B.; Owston, P. G. *Acta Crystallogr.* **1969**, *B25*, 1753.

(17) (a) Francis, J. N.; McAdam, A.; Ibers, J. A. *J. Organomet. Chem.* **1971**, *29*, 231. (b) Francis, J. N.; McAdam, A.; Ibers, J. A. *J. Organomet. Chem.* **1971**, *29*, 131. (c) McAdam, A.; Francis, J. N.; Ibers, J. A. *J. Organomet. Chem.* **1971**, *29*, 149. (d) Panattoni, C.; Graziani, R.; Belluco, U.; Baddley, W. H. Cited in Marnojlovic-Muir, L.; Muir, K. W.; Ibers, J. A. *Discuss. Farad. Soc.* **1969**, *47*, 84.

Table I. Bond Distances (Å) of C–C, Si–C, and Si–Si in $Pt(PH_3)_2L$ and $[PtCl_3L]^-$ (L = C_2H_4, SiH_2CH_2, Si_2H_4)

	CH_2=CH_2	SiH_2=CH_2	SiH_2=SiH_2
free XH_2=$X'H_2$	1.315	1.703	2.127[a]
free XH_3–$X'H_3$	1.550	1.907	2.377
in $Pt(PH_3)_2L$	1.411 (41%)[b]	1.823 (59%)	2.252 (50%)
in $[PtCl_3L]^-$	1.358 (18%)	1.786 (41%)	2.224 (39%)

[a] Trans-bending structure of the free Si_2H_4 molecule. [b] In parentheses is given the percentage of the ratio going to a single bond from a double bond.

extent as observed by experiment in which the C=C bond lengthens by 0.038 Å upon C_2H_4 coordination.[16a] Unfortunately, however, optimized bond distances of Pt–C, Pt–Cl, and Pt–P are slightly longer than the corresponding experimental values (see Figure 1).[16,17] The Pt–C distance hardly shortens upon introducing electron correlation, as will be described later. Thus, some other factor is considered to be the reason that these optimized distances are longer than their experimental values. Another small discrepancy is also found; the trans Pt–Cl bond of $[PtCl_3(C_2H_4)]^-$ is calculated to lengthen upon coordination of C_2H_4 (compare Figure 1 and Figure 2), but it is still slightly shorter than the cis Pt–Cl bond, while the trans Pt–Cl bond is experimentally reported to be slightly longer than the cis Pt–Cl bond.[16] The Pt–Cl bond includes a bonding interaction between the occupied p_σ orbital of Cl and the vacant orbitals of Pt and an antibonding interaction between the occupied p_π orbital of Cl and the occupied d_π orbital of Pt. If the donating interaction of C_2H_4 is strong, the trans Cl ligand can not effectively donate its p_σ electrons to vacant orbitals of Pt, which weakens the Pt–Cl bond. However, if the back-bonding to C_2H_4 is strong, the Pt d_π–Cl p_π antibonding interaction is weakened, which favors the trans Pt–Cl bond. Thus, the σ-donating and π-back-donating interactions of C_2H_4 have a reverse effect on the strength of the trans Pt–Cl bond. This means that the relative strength of trans Pt–Cl and cis Pt–Cl bonds is sensitive to the Pt–C_2H_4 interaction. This is probably one of the reasons that a small discrepancy is found in the relative distances of trans Pt–Cl and cis Pt–Cl between experiment and calculations. Furthermore, the K^+ ion which exists near the trans Cl ligand is considered to lengthen the trans Pt–Cl bond.[16a] MO calculations would tend to underestimate the lengthening of the trans Pt–Cl bond, because the K^+ ion is not included in the calculation.[3] Thus, the calculated result where the trans Pt–Cl bond is slightly shorter than the cis Pt–Cl bond does not seem unreasonable.

Although a few discrepancies between calculations and experiments are found as described above, the Pt–Si, Si=C, and Si=Si distances and CH_2 and SiH_2 back-bending angles of $Pt(PH_3)_2(Si_2H_4)$ and $Pt(PH_3)_2(SiH_2CH_2)$ roughly agree with those of similar low-valent transition-metal complexes of silene and disilene.[18-20] Therefore, coordinate bonds of ethylene, silene, and disilene would be compared semiquantitatively, at least, in the present theoretical calculations. Several interesting results are found in such a comparison. The first to be discussed is the bond lengthening of C=C, Si=C, and Si=Si caused by coordination. As shown in Table I, the Si–C distance in $Pt(PH_3)_2(SiH_2CH_2)$ is slightly longer than an average of Si—C single and Si=C double bonds. The Si–Si distance in $Pt(PH_3)_2(Si_2H_4)$ is almost the same as an average of Si—Si single and Si=Si double bonds. On the other hand, the C–C distance in $Pt(PH_3)_2(C_2H_4)$ is slightly shorter

Chart II

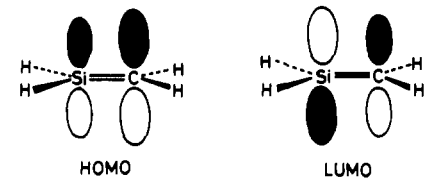

Chart III

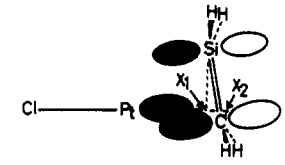

Table II. Electron Correlation Effects on Some Important Geometrical Parameters[a] of $Pt(PH_3)_2L$ (L = C_2H_4, Si_2H_4)

	HF	MP2	MP3	MP4(DQ)	MP4(SDQ)
			$Pt(PH_3)_2(C_2H_4)$		
R(Pt–C)	2.16	2.17	2.16	2.17	2.18
R(C–C)	1.42	1.45	1.45	1.45	1.45
Θ[b]	156	156	155	156	156
			$Pt(PH_3)_2(Si_2H_4)$		
R(Pt–Si)	2.42	2.41	2.41	2.42	2.42
R(Si–Si)	2.26	2.26	2.28	2.27	2.27
Θ[b]	156	156	156	156	156
			free C_2H_4		
R(C–C)	1.353	1.377	1.374	1.376	1.377
			free SiH_2H_4		
R(Si–Si)[c]	2.277	2.316	2.317	2.315	2.323

[a] In Å for bond distances and in deg for bond angles. See ref 22 for the optimization procedure. [b] Back-bending angle. [c] The trans-bending angle of the SiH_2 plane (25.7°) is optimized at the MP2 level.

than an average of C—C single and C=C double bonds. In the Pt(II) complexes, bond lengthening is smaller than in Pt(0) complexes. The next feature to be noted is the trans-influence effect of Si compounds. In $Pt(PH_3)_2(SiH_2CH_2)$, the Pt–P bond transpositioned to the Si atom is longer than the Pt–P bond transpositioned to the C atom (see Figure 1). In $[PtCl_3L]^-$, the strong trans-influence effect of Si compounds is more clearly observed. Although the cis Pt–Cl bond distance hardly depends on the L ligand, the trans Pt–Cl bond becomes longer in the oder $[PtCl_3(C_2H_4)]^- < [PtCl_3(SiH_2CH_2)]^- < [PtCl_3(Si_2H_4)]^-$. From these results, we can conclude that Si compounds have a stronger trans-influence effect than C compounds. This strong trans-influence effect of Si compounds would result from their strong donating ability, as will be discussed later. The third point is that the coordination structure of $[PtCl_3(SiH_2CH_2)]^-$ significantly deviates from C_{2v} symmetry unlike the other complexes; the C atom is located at the trans position of the Cl ligand, while the Si atom avoids the trans position. The HOMO of SiH_2CH_2 has a greater contribution from the C p_π orbital than from the Si p_π orbital, while its LUMO has a smaller contribution from the C p_π orbital than from the Si p_π orbital (see schematic picture in Chart II), due to the smaller electronegativity of Si compared to C. Because the vacant Pt dσ orbital expands to the trans-position of the Cl ligand as shown in Chart III, this unsymmetrical structure results in better overlap between the Pt d_σ orbital and the large p_π orbital of C than the symmetrical structure. The energy difference between this unsymmetrical structure and the nearly symmetrical one is, however, very small.[21] This suggests

(18) Only a rough comparison is possible here because the central metal is different between the present theoretical and the experimental works.

(19) (a) Geometrical parameters of $Pt(PH_3)_2(SiH_2CH_2)$ might be compared with R(Ru–Si) = 2.382, 2.365 Å, R(Ru–C) = 2.25, 2.26 Å, and R(Si–C) = 1.78, 1.79 Å of $(\eta^5\text{-}C_5Me_5)(PPr^i_3)Ru(H)(\eta^2\text{-}CH_2SiPh_2)$[19b] and R(Ir–Si) = 2.317 Å, R(Ir–C) = 2.189 Å, the CH_2 back-bending angle = 162.7°, and the $SiPh_2$ back-bending angle = 140.8° of $(\eta^5\text{-}C_5Me_5)(PMe_3)Ir(SiPh_2CH_2)$.[19c] (b) Campion, B. K.; Heyn, R. H.; Tilley, T. D. *J. Am. Chem. Soc.* **1988**, *110*, 7558. (c) Campion, B. K.; Heyn, R. H.; Tilley, T. D. *J. Am. Chem. Soc.* **1990**, *112*, 4079.

(20) (a) Geometrical parameters of $Pt(PH_3)_2(Si_2H_4)$ might be compared with R(W–Si) = 2.606 Å and R(Si–Si) = 2.260 Å of $W(\eta^5\text{-}C_5H_5)(Si_2Me_4)$.[20b] (b) Berry, D. H.; Chey, J. H.; Zipin, H. S.; Carroll, P. J. *J. Am. Chem. Soc.* **1990**, *112*, 452.

(21) The nearly symmetrical coordinate structure has been optimized under the assumption that the Si–X_1 distance is the same as the C–X_2 distance (see Chart III for X_1 and X_2). The unsymmetrical structure is more stable than the nearly symmetrical one by ca. 1.7 kcal/mol at the Hartree–Fock level and 1.2 kcal/mol at the MP4(SDQ) level.

Table III. Binding Energies (kcal/mol) of Ethylene, Silene, and Disilene Coordination to $Pt(PH_3)_2$ and $[PtCl_3]^-$

	HF	MP2	MP3	MP4-(DQ)	MP4-(SDQ)	SD-CI[a]
$Pt(PH_3)_2(C_2H_4)$	2.5	25.8	17.9	19.2	20.3	10.6
$Pt(PH_3)_2(SiH_2CH_2)$	35.3	55.5	48.2	32.5	42.8	
$Pt(PH_3)_2(Si_2H_4)$	52.5	75.8	65.5	68.9	70.3	57.3
$[PtCl_3(C_2H_4)]^-$	18.2	37.1	31.4	31.8	32.8	26.7
$[PtCl_3(SiH_2CH_2)]^-$	42.3	72.7	62.6	65.2	66.3	
$[PtCl_3(Si_2H_4)]^-$	54.7	93.9	78.6	83.8	86.1	71.8

[a] This value was calculated as the energy difference of E(est full CI) between the equilibrium structure of the complex and the infinitely separated structure in which a distance between Pt and the center of E=E bond (E = S, Si) was taken to be 50 Å.

that the coordination structure of silene complexes is sensitive to the central metal.

Electron Correlation Effects on Geometry. Electron correlation effects on geometry were investigated with MP2–MP4 methods in $Pt(PH_3)_2L$,[22] because these complexes have a strong π-back-bonding interaction (note that the π-back-bonding cannot be described well at the Hartree–Fock level but is improved by introducing electron correlation in general).[23] As shown in Table II the Pt–Si distance hardly lengthens upon introducing electron correlation, while the Pt–C distance slightly lengthens. Also the back-bending angles of both CH_2 and SiH_2 planes are hardly changed by electron correlation. The C=C distance in $Pt(PH_3)_2(C_2H_4)$ lengthens upon introducing electron correlation to a degree similar to that for the free C_2H_4 molecule. This result seems reasonable because electron correlation generally lengthens the covalent bond.[24] On the other hand, introduction of electron correlation hardly lengthens the Si=Si distance in $Pt(PH_3)_2(Si_2H_4)$, whereas it considerably lengthens the Si=Si distance in the free Si_2H_4 molecule. This result is counter to our expectation. One of possible reasons is that contribution of the intraligand π–π^* excited configuration of Si_2H_4 is smaller in the Pt(0) complex than in the free Si_2H_4 molecule, as described later.

In conclusion, electron correlation effects on geometry are unexpectedly small in Pt–Si compounds, and the geometry optimization at the Hartree–Fock level seems reasonable in investigating Pt–Si interaction.

Binding Energies of Ethylene, Silene, and Disilene Complexes. Binding energy is defined as a stabilizing energy caused by coordination of these ligands to Pt(0) or Pt(II). Compared to the Hartree–Fock level, introduction of electron correlation significantly increases binding energies, as shown in Table III. This means that inclusion of electron correlation is indispensable in discussing energetics, whereas correlation effects on geometry are rather small.

Unfortunately, the binding energy at the correlated level depends on the calculational methods. However, the difference in binding energy between $Pt(PH_3)_2(C_2H_4)$ and $Pt(PH_3)_2(Si_2H_4)$ is little influenced by the method; the difference is calculated to be about 50 kcal/mol with the MP4(SDQ) method and 47 kcal/mol with the SD–CI method. Also, the difference in binding energy between $[PtCl_3(C_2H_4)]^-$ and $[PtCl_3(Si_2H_4)]^-$ is calculated to be 54 kcal/mol with the MP4(SDQ) method and 47 kcal/mol with the SD–CI method. These results suggest that binding energies of ethylene, silene, and disilene complexes can be reliably compared with each other. The silene coordination is estimated to be stronger than the ethylene coordination by about 20 kcal/mol in the Pt(0) complexes and by about 34 kcal/mol in the Pt(II) complexes. The disilene coordination is furthermore stronger than the silene coordination by about 30 kcal/mol in the Pt(0) complexes and by about 20 kcal/mol in Pt(II) complexes. The strong coordinate bond of silene has been suggested by the experimental fact that the silene complex $Cp^*(PR_3)Ir(I)(\eta^2\text{-}SiH_2{=}CH_2)$ cannot be decomposed even at 140 °C.[19c]

Table IV. Occupation Numbers of Some Important Natural Orbitals

$Pt(PH_3)_2(C_2H_4)$			50-Å separated str[a]		
orbital	occ no.	character	orbital	occ no.	character
$11b_1$	1.973	(Pt d_π–C_2H_4 π^*)[b]	$8b_1$	1.985	Pt d_π
$15a_1$	1.973	C_2H_4 π	$15a_1$	1.953	C_2H_4 π
$12b_1$	0.036	(C_2H_4 π^*–Pt d_π)[a]	$12b_1$	0.042	C_2H_4 π^*
$17a_1$	0.015	(Pt d_σ–C_2H_4 π)[a]	$17a_1$	0.006	Pt d_σ
$Pt(PH_3)_2(Si_2H_4)$			50-Å separated str		
orbital	occ no.	character	orbital	occ no.	character
$17a_1$	1.976	Si_2H_4 π, Pt s	$17a_1$	1.989	Si_2H_4 σ(p)
$14b_1$	1.974	(Pt dπ–Si_2H_4 π^*)[b]	$11b_1$	1.989	Pt d_π
$18a_1$	1.967	Si_2H_4 π and σ	$18a_1$	1.945	Si_2H_4 π
$15b_1$	0.029	(Si_2H_4 π^*–Pt d_π)[a]	$15b_1$	0.045	Si_2H_4*
$[PtCl_3(C_2H_4)]^-$			50-Å separated str		
orbital	occ no.	character	orbital	occ no.	character
$8b_1$	1.982	(Pt dπ–C_2H_4 π^*)[b]	$7b_1$	1.990	Pt dπ
$19a_1$	1.962	(C_2H_4 π–Pt d_σ)[b]	$19a_1$	1.950	C_2H_4 π
$9b_1$	0.035	(C_2H_4 π^*–Pt d_π)[a]	$9b_1$	0.044	C_2H_4 π^*
$[PtCl_3(Si_2H_4)]^-$			50-Å separated str		
orbital	occ no.	character	orbital	occ no.	character
$11b_1$	1.975	(Pt d_π–Si_2H_4 π^*)[b]	$10b_1$	1.989	Pt dπ
$22a_1$	1.963	Si_2H_4 π	$22a_1$	1.944	Si_2H_4 π
$12b_1$	0.033	(C_2H_4 π^*–Pt d_π)[a]	$12b_1$	0.040	Si_2H_4 π^*

[a] Structures of C_2H_4 and Si_2H_4 are distorted as in the complex.

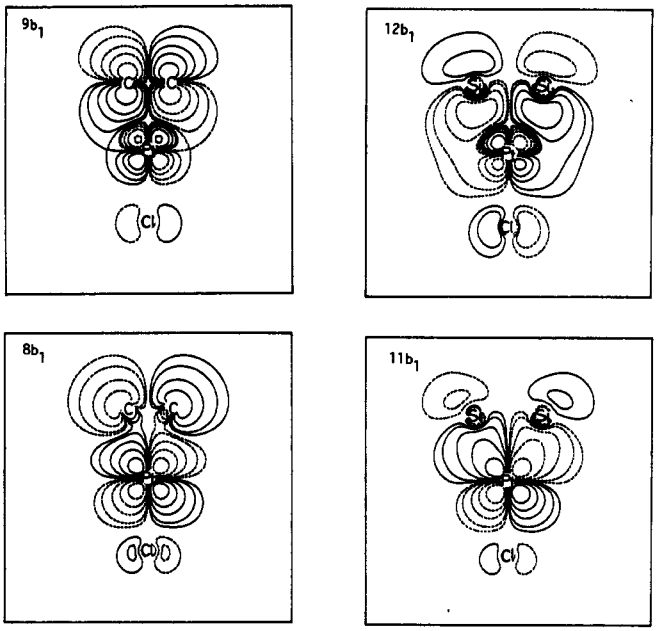

Figure 3. Contour maps of important natural orbitals of $[PtCl_3(C_2H_4)]^-$ and $[PtCl_3(Si_2H_4)]^-$ at the SD-CI level. Values of contours: ±0.2, ±0.1, ±0.05, ±0.02, ±0.01.

The Nature of Electron Correlation. The nature of electron correlation is examined here, based on occupation numbers of several important natural orbitals.[25] Natural orbitals whose occupation numbers are considerably different between the Pt complex and the infinitely separated structure are considered important to the coordinate bond and they are listed in Table IV. In the infinitely separated structure, the occupation number of the π orbital considerably decreases from 2.0 but that of the π^*

(22) The optimized values are estimated independently by using parabolic fitting of total energies, where the other geometrical parameters were fixed to optimized values by the energy gradient technique at the Hartree–Fock level.
(23) McMichael, C.; Hay, P. J. *J. Am. Chem. Soc.* **1985**, *83*, 4641.
(24) Hehre, W. J.; Radom, L.; Schleyer, P. v. R.; Pople, J. A. *Ab initio Molecular Orbital Theory*; John Wiley: New York, 1986; p 162.
(25) Discussion based on the CI expansion coefficients is difficult because many small CI expansion coefficients contribute to the total wave function.

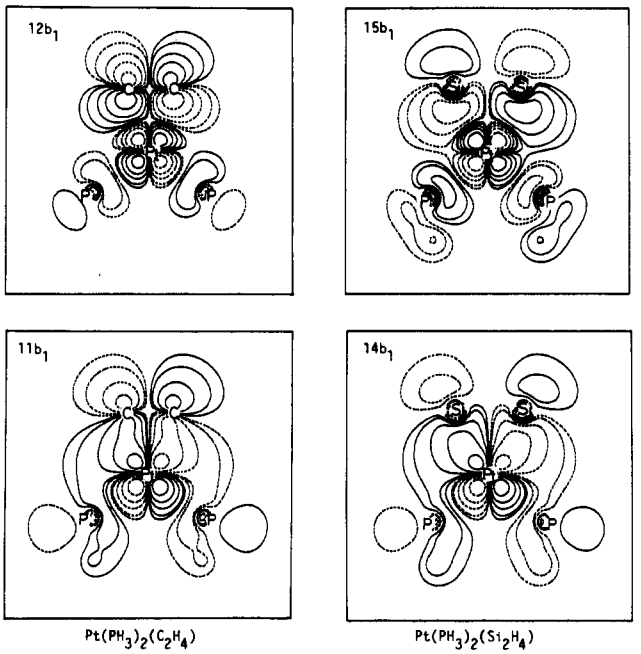

Figure 4. Contour maps of important natural orbitals of $Pt(PH_3)_2(C_2H_4)$ and $Pt(PH_3)_2(Si_2H_4)$ at the SD–CI level. See Figure 3 for the values of contours.

orbital remarkably increases from 0.0, which indicates that the π–π^* excited configuration is important. In both the Pt(0) and Pt(II) complexes, the occupation number of the (Pt d_π–L π^*)^b orbital[26] considerably decreases from 2.0 but that of (L π^*–Pt d_π)^a remarkably increases from 0.0, which suggests that the (Pt d_π–L π^*)^b → (L π^*–Pt d_π)^a excited configuration is important along with the intraligand π–π^* excited configuration. The (Pt d_π–L π^*)^b and (L π^*–Pt d_π)^a orbitals are shown in Figures 3 and 4. Apparently, the former involves the π-back-bonding interaction between Pt d_π and L π^* orbitals as a main contributor, and the latter, its antibonding counterpart. This means that electron correlation improves the π-back-bonding interaction between Pt and L as in $Ni(PH_3)_2(N_2)$[27a] and $Ni(PH_3)_2(CO_2)$.[27b] On the other hand, a contribution of the intraligand π–π^* excited configuration decreases upon going to the Pt complexes from the infinitely separated structure, as is clearly indicated by the larger occupation number of the L π orbital in the complex than in the infinitely separated structure. Such decrease in the intraligand π–π^* excited configuration is considered to be one of the reasons that electron correlation hardly lengthens the Si=Si distance in $Pt(PH_3)_2(Si_2H_4)$ but lengthens it in the free Si_2H_4 molecule. However, the occupation numbers of Table IV cannot offer a clear reason that electron correlation lengthens the C=C distance in $Pt(PH_3)_2(C_2H_4)$ but hardly lengthens the Si=Si distance in $Pt(PH_3)_2(Si_2H_4)$. This difference between ethylene and disilene complexes should be investigated in more detail in the future.

Electron Distribution and Coordinate Bond Nature. Electron distribution is examined briefly, based first on Mulliken populations (Table V). In both Pt(0) and Pt(II) complexes, the Pt d_π orbital population decreases upon coordination of L, and its decrease becomes larger in the order $C_2H_4 < SiH_2CH_2 < Si_2H_4$, which means that the π-back-bonding interaction becomes stronger in this order. In Pt(0) complexes, electron populations of C_2H_4 and SiH_2CH_2 increase upon their coordinatioin to Pt(0), and their increases become smaller in the order $C_2H_4 > SiH_2CH_2$. On the other hand, the electron population of Si_2H_4 decreases upon its coordination to Pt(0). In Pt(II) complexes, the electron population

(26) The representation $(\chi_1 - \chi_2)^{a(or\ b)}$ means that the χ_1 orbital contributes more to this interaction than the χ_2 orbital. The superscript "a" means the antibonding interaction between χ_1 and χ_2, and the superscript "b", its bonding interaction.

(27) (a) Sakaki, S.; Ohkubo, K. *J. Phys. Chem.* **1989**, *93*, 5655. (b) Sakaki, S.; Koga, N.; Morokuma, K. *Inorg. Chem.* **1990**, *29*, 3110.

Table V. Changes in Mulliken Population[a] Caused by Coordination of L (L = Ethylene, Silene, Disilene) to $Pt(PH_3)_2$ and $[PtCl_3]^-$

	$Pt(PH_3)_2L$			$[PtCl_3L]^-$		
	C_2H_4	SiH_2CH_2	Si_2H_4	C_2H_4	SiH_2CH_2	Si_2H_4
Pt	−0.023	0.131	0.299	0.153	0.280	0.446
d	−0.399	−0.417	−0.444	−0.152	−0.190	−0.332
L	0.164	0.102	−0.034	−0.199	−0.260	−0.408
X trans[c]	−0.060	−0.098	−0.131	0.058	0.070	0.091
X cis		−0.135		−0.006	−0.045	−0.115

[a] A positive value means an increase in population by coordination of L and vice versa. These values are calculated at the Hartree–Fock level with the BS-II basis. [b] In the case of silene complexes, the dπ orbital can not be defiend. However, the d_{xz} orbital (see Figure 1 for the coordinate system) plays the role of donating d_π orbital as in ethylene and disilene complexes; this orbital is doubly occupied in $Pt(PH_3)_2$ and $[PtCl_3]^-$ and donates its electrons to the π^* orbital of silene. [c] X = PH_3 or Cl. "Trans" means the trans-position to the Si atom in $Pt(PH_3)_2(SiH_2CH_2)$ and that to the L ligand in $[PtCl_3L]^-$.

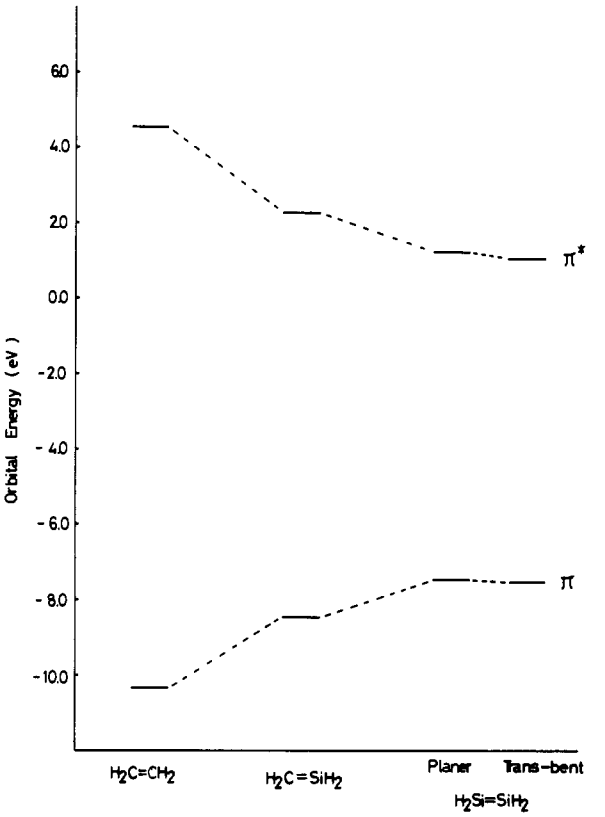

Figure 5. π and π^* orbital energies of ethylene, silene, and disilene. The MIDI-4 set was used. Geometries were optimized at the Hartree–Fock level.

of all these ligands decreases upon coordination, and their decreases become larger in the order $C_2H_4 < SiH_2CH_2 < Si_2H_4$. These results indicate that both σ-donation and π-back-bonding interactions become stronger in this order. The Pt atomic population of both Pt(0) and Pt(II) complexes increases in the same order, which indicates that the σ-donating interaction becomes stronger in this order to a greater extent than the π-back-bonding interaction does.

The strength of σ-donation and π-back-donating interactions depends on the energy levels of π and π^* orbitals. The π orbital raises in energy and the π^* orbital lowers in energy in the order $C_2H_4 < SiH_2CH_2 < Si_2H_4$, as shown in Figure 5. This is the reason that both σ-donating and π-back-bonding interactions become stronger in this order.

The electron distribution of the ethylene and disilene complexes is now investigated in more detail, based on difference density maps at the correlated level, as shown in Figures 6–9. Since these complexes have C_{2v} symmetry, the electron density can be divided into several components related to either σ-donation or π-back-

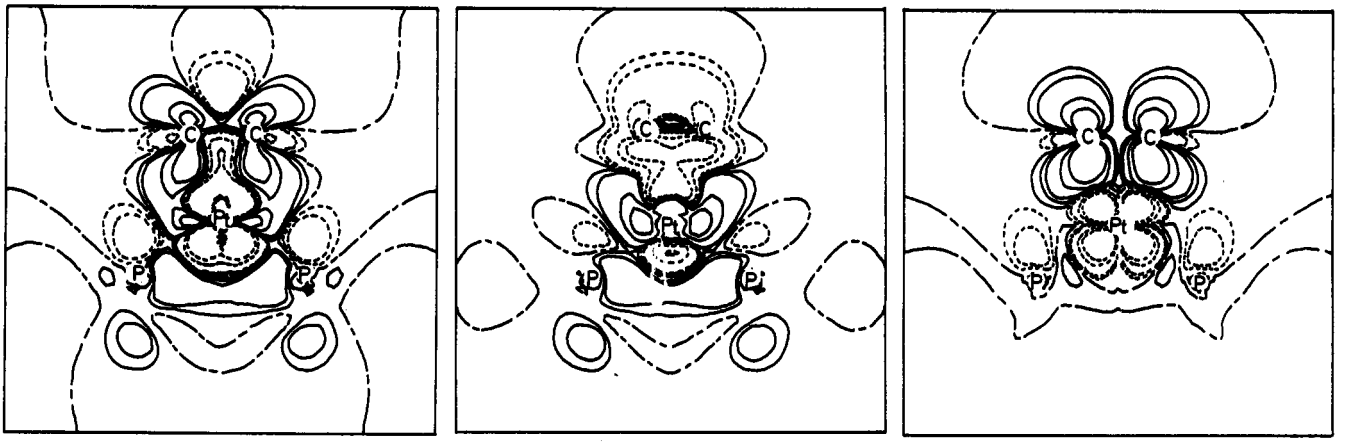

Figure 6. Difference density maps of $Pt(PH_3)_2(C_2H_4)$ at the SD–CI level. Key: $\Delta\rho = \rho[Pt(PH_3)_2(C_2H_4)] - \rho[Pt(PH_3)_2] - \rho[C_2H_4]$; solid lines indicate increase in density; dashed lines; indicate decrease in density; the –·– line indicates 0.0; contour values are ±0.01, ±0.005, ±0.001, ±0.0005, and 0.0.

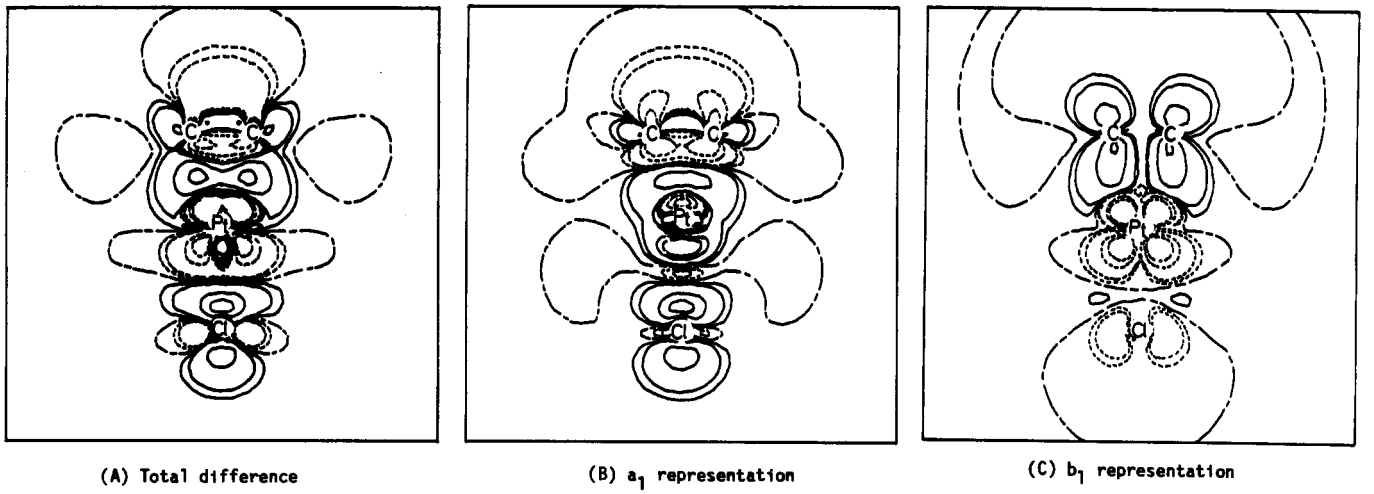

Figure 7. Difference density maps of $[PtCl_3(C_2H_4)]^-$ at the SD-CI level. The key is the same as in Figure 6.

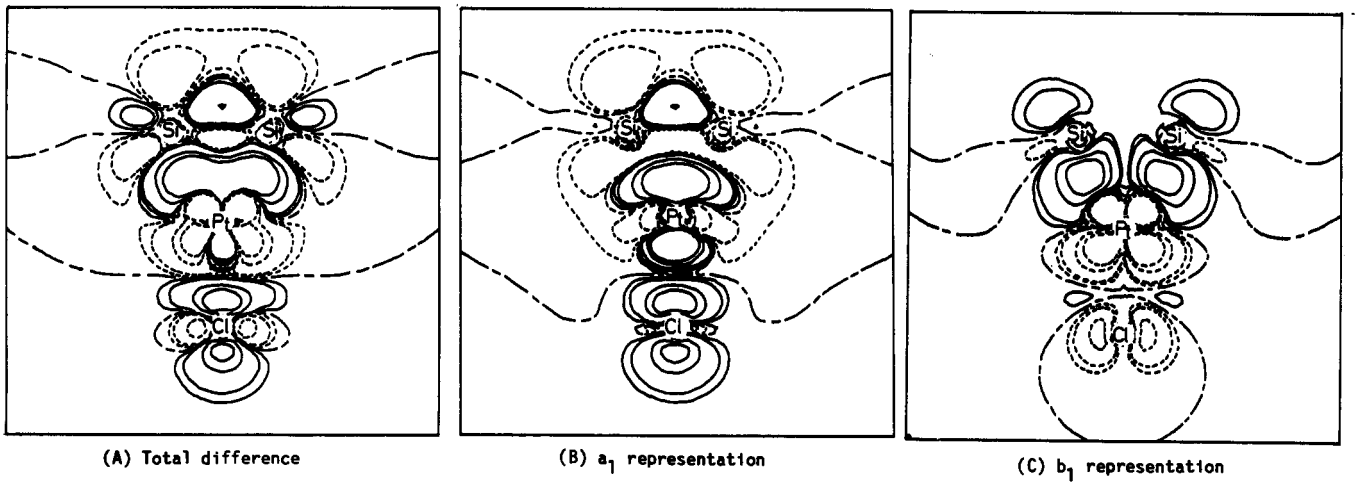

Figure 8. Difference density maps of $[PtCl_3(Si_2H_4)]^-$ at the SD-CI level. The key is the same as in Figure 6.

donation;[28] the difference density in the a_1 representation indicates electron redistribution caused by σ-donation, and that in the b_1 representation shows electron redistribution caused by π-back donation because the σ-donation and π-back donation are included in the a_1 and b_1 representations, respectively.

In $Pt(PH_3)_2(C_2H_4)$, total difference density decreases around the Pt atom but increases around two C atoms (Figure 6), suggesting that the π-back-bonding is important. In $[PtCl_3(C_2H_4)]^-$, electron density decreases around both ethylene and Pt (Figure 7), which indicates that the σ-donation contributes to the coordinate bond to a similar extent to the π-back-bonding. These features are in accordance with the results from Mulliken populations.[29] In both $Pt(PH_3)_2(C_2H_4)$ and $[PtCl_3(C_2H_4)]^-$, the

(28) The silene complex has a lower C_1, symmetry, and electron density cannot be divided into the representations related to either σ-donation or π-back-bonding. Furthermore the SD–CI calculations of silene complexes are quite time-consuming, because of low symmetry. Thus, the difference density of the silene complex is not calculated here, and the ethylene and disilene coordinate bonds are discussed as typical examples.

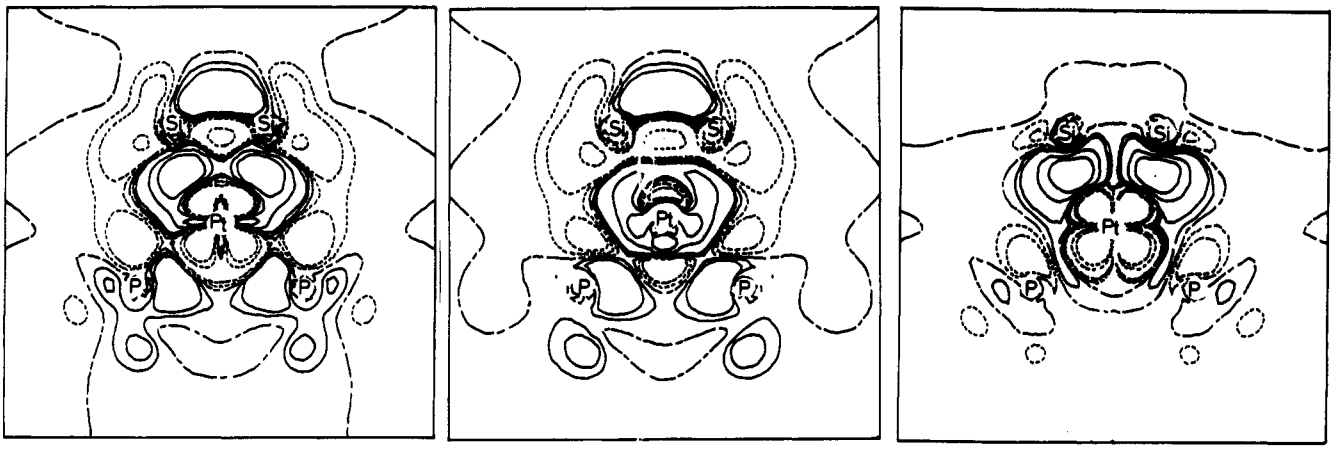

Figure 9. Difference density maps of $Pt(PH_3)_2(Si_2H_4)$ at the SD-CI level. The key is the same as in Figure 6.

electron density of the a_1 representation decreases around ethylene but increases around the Pt atom, which clearly indicates the character of the σ-donating interaction. In the b_1 representation, electron density increases around ethylene but decreases in the Pt d_π orbital region, which clearly shows a characteristic feature of the π-back-bonding interaction. Thus, the coordinate bond of ethylene can be described well by the Dewar–Chatt–Duncanson model in these complexes. This electron redistribution indicates that the C_2H_4 coordinate bond can be described by C=C double-bond coordination (Chart IA) because charge accumulation on the ethylene π^* orbital is clearly shown in Figures 7C and 8C. The charge transfer arising in the b_1 representation is larger in $Pt(PH_3)_2(C_2H_4)$ than in $[PtCl_3(C_2H_4)]^-$, while the charge transfer arising in the a_1 representation is smaller in the former than in the latter. These results agree with our expectation that σ-donation is stronger but π-back-donation is weaker in the Pt(II) complex than in the Pt(0) complex.

In $[PtCl_3(Si_2H_4)]^-$, electron redistribution is similar to that of the ethylene analogue (Figure 8), which means that the coordinate bond of this complex might be characterized in terms of coordination of the Si=Si double bond. A difference between $[PtCl_3(Si_2H_4)]^-$ and its ethylene analogues is, of course, found. In the disilene complex, charge accumulation between Pt and Si_2H_4 is greater than in the ethylene analogue (compare Figure 7 with Figure 8). This result is in accordance with the stronger coordinate bond of disilene than that of ethylene.

$Pt(PH_3)_2(Si_2H_4)$ shows a critically different electron distribution from the others discussed above (Figure 9). In the total difference density map, electron density significantly accumulates between Pt and two Si atoms, and considerably decreases in the σ-bond region of the Si–Si bond. In the a_1 representation, electron density decreases around Si_2H_4, but increases near the Pt atom. This electron redistribution corresponds to the charge transfer from Si_2H_4 to Pt, while a picture of charge transfer from the Si_2H_4 π orbital to vacant orbitals of Pt cannot be found in this figure. In the b_1 representation, more interesting electron redistribution occurs. Electron density significantly decreases in the Pt d_π orbital region. This electron distribution indicates that the back-bonding from the Pt d_π orbital to Si_2H_4 significantly participates in the coordinate bond. However, electron density accumulates not in the Si_2H_4 π^* orbital but between Pt and two Si atoms. Also, contour maps of Figures 3 and 4 indicate interesting differences in the coordinate bond between ethylene and disilene. In the $12b_1$ MO of $Pt(PH_3)_2(C_2H_4)$ and the $9b_1$ MO of $[PtCl_3(C_2H_4)]^-$, existence of the π^* orbital is clearly observed. In the $15b_1$ MO of $Pt(PH_3)_2(Si_2H_4)$, on the other hand, the π^* orbital is significantly deformed; remarkably high contours are found between Pt and Si atoms, but substantially low contours are found on the back side of disilene. These results suggest that the Pt–Si bond has the character of a considerably large covalent interaction. Thus, the disilene coordinate bond of $Pt(PH_3)_2(Si_2H_4)$ cannot be considered as coordination of a Si=Si double bond (Chart IA) but is instead a metallocyclopropane-type interaction (Chart IB).

Finally, the origin of the trans-influence effect of ethylene and disilene is discussed, based on the difference density maps. In both $[PtCl_3(C_2H_4)]^-$ and $[PtCl_3(Si_2H_4)]^-$, coordination of ethylene and disilene increases electron density on the trans Cl ligand and an increase of density is larger in $[PtCl_3(Si_2H_4)]^-$ than in $[PtCl_3(C_2H_4)]^-$, as shown in Figures 8A and 9A and in Table V. This means that charge transfer from the trans Cl ligand to Pt is weakened by coordination of ethylene and disilene and that its weakening is larger in $[PtCl_3(Si_2H_4)]^-$ than in $[PtCl_3(C_2H_4)]^-$. The charge accumulation on the trans Cl ligand arises mainly in the a_1 representation, which includes the σ-donating interaction from ethylene to Pt as a main contributor. Thus, the trans-influence effect of these ligands arises from the σ-donating interaction, and the stronger trans-influence effect of disilene than that of ethylene would result from the large donating ability of disilene.

Concluding Remarks. Although optimization of $Pt(PH_3)_2L$ and $[PtCl_3L]^-$ (L = C_2H_4, SiH_2CH_2, Si_2H_4) yields longer Pt–Cl, Pt–C, and Pt–P bond distances than the corresponding experimental values, coordinate structures of silene and disilene can be reliably compared with that of ethylene. Electron correlation scarcely influences geometrical parameters but significantly influences the binding energy. The relative strength of coordinate bonds is estimated at the correlated level; the coordinate bond of silene is stronger than that of ethylene by about 20 kcal/mol in the Pt(0) complex and by about 34 kcal/mol in the Pt(II) complex. The coordinate bond of disilene is furthermore stronger than the coordinate bond of silene by about 30 kcal/mol in the Pt(0) complex and by about 20 kcal/mol in the Pt(II) complex. The coordinate bonds of ethylene with Pt(0) and Pt(II) and that of disilene with Pt(II) exhibit a considerable amount of the character of C=C or Si=Si double-bond coordination and they can be described by the Dewar–Chatt–Duncanson model. On the other hand, the coordinate bond of disilene with Pt(0) can be described as the metallocyclopropane-type interaction.

Acknowledgment. These calculations were carried out with the Hitac M-680 and S-820 computers of Institute for Molecular Science (Okazaki, Japan).

Registry No. $PtCl_3C_2H_4$, 136174-28-2; $PtCl_3SiH_2CH_2$, 136174-30-6; $PtCl_3Si_2H_4$, 136174-32-8; $Pt(PH_3)_2C_2H_4$, 31941-73-8; $Pt(PH_3)_2SiH_2CH_2$, 136174-29-3; $Pt(PH_3)_2Si_2H_4$, 136174-31-7.

(29) The ethylene coordination to $[PtCl_3]^-$ decreases the d orbital population by about 0.15 and the C_2H_4 electron population by about 0.20 (Table V), which accords with a decrease in electron density around Pt and C_2H_4. Although the density decreases near Pt, the Pt atomic population increases. This increase results from an increase in the Pt 6p orbital population, which probably corresponds to the charge accumulation between Pt and C_2H_4 becauise the 6p orbital expands far from Pt.